The Journal of Physical Chemistry B

 VOLUME 103, NUMBER 50, DECEMBER 16, 1999

LETTERS

EPR on Biological Samples beyond the Limits of Superconducting Magnets—The Primary Donor Cation of Purple Bacterial Photosynthesis

Peter J. Bratt,[†] Erin Ringus,[‡] Alia Hassan,[§] Hans Van Tol,[§] Anna-Lisa Maniero,[§,||] Louis-Claude Brunel,[§] Martin Rohrer,[§,⊥] Claudia Bubenzer-Hange,[#] Hugo Scheer,[#] and Alexander Angerhofer*[,†]

Department of Chemistry, University of Florida, Box 117200, Gainesville, Florida 32611, Department of Science, Columbia College, Box 481, Columbia, South Carolina 29203, National High Magnetic Field Laboratory, Center for Interdisciplinary Magnetic Resonance, 1800 E. Paul Dirac Drive, Tallahassee, Florida 32310, Dipartimento di Chimica Fisica, Università di Padova, Via Loredan 2, I-35131 Padova, Italy, Institut für Physikalische und Theoretische Chemie, J. W. Goethe-Universität Frankfurt, Marie-Curie Str. 11, D-60439 Frankfurt a. M., Germany, Botanisches Institut, Universität München, Menzinger Strasse 67, D-80638 München, Germany

Received: August 16, 1999; In Final Form: October 11, 1999

The *g*-matrix of a free radical is an important observable that yields information on its electronic structure. It is usually measured by electron paramagnetic resonance (EPR) under "high field" conditions, where the spectral splitting of the principal *g*-factor components is larger than the line width due to unresolved hyperfine splitting. For large organic molecules such as the primary electron donor in photosynthetic reaction centers (RC) this usually requires fields above 11 T, or, for fields between 3 and 11 T, full deuteration and/or single-crystal work. When trying to obtain improved spectral resolution a major concern is the presence of *g*-strain which leads to extra line broadening. Here we show that *g*-strain is negligible for bacterial RCs up to a field of 24 T. We investigated the temperature dependence of the *g*-anisotropy for RCs from *Rhodobacter* (*Rb.*) *sphaeroides* using different detergents and find that within experimental errors there is no change in the principal *g*-matrix components up to 200 K. This is the first report of a successful EPR experiment on a biological sample above the limits of superconducting magnets.

1. Introduction

Electron transfer in bacterial photosynthesis is controlled by the spatial and electronic structure of the cofactors within the RC. Its spatial structure is comprised of three protein subunits, the L, M, and H chains, which contain the electron transfer-active cofactors: two bacteriochlorophyll (BChl) molecules which form the special pair primary donor, P_{865}, two accessory BChl's, two bacteriopheophytin (BPh) molecules, two quinone acceptors, a non-heme iron atom, and in the case of the wild-type RCs, a spheroidene molecule which acts to protect the RC from photooxidation.[1,2] The electronic structure of $P_{865}^{+\bullet}$ from *Rhodobacter* (*Rb.*) *sphaeroides* has been studied extensively by EPR and Electron Nuclear DOuble Resonance (ENDOR)

* Author to whom correspondence should be addressed at Chemistry Department, University of Florida, Gainesville, FL 32611. Phone: (352) 846-3281. Fax: (352) 392-0872. E-mail: alex@chem.ufl.edu.
[†] University of Florida.
[‡] Columbia College.
[§] Center for Interdisciplinary Magnetic Resonance.
[||] On leave from Università di Padova.
[⊥] J. W. Goethe-Universität Frankfurt.
[#] Universität München.

10.1021/jp992885a CCC: $18.00
Published on Web 11/24/1999

spectroscopy.[3] These studies have shown that under physiological conditions the unpaired electron is distributed asymmetrically over the two halves of the dimer with a 2:1 electron distribution ratio in favor of the D_A molecule while at cryogenic temperatures another conformation exists with a more monomeric spin distribution of about 5:1.[4] This asymmetry in the electron distribution ratio is almost certainly due to interaction of the protein matrix with the two BChl molecules of the primary donor and, to some extent, to slight asymmetries in the primary donor structure itself, such as different extents of ring puckering and differing rotational angles of the two acetyl groups. It may have a functional role in the efficient charge transfer of the electron from the primary donor.[5] An alternative approach to characterizing the electronic structure of $P_{865}^{+\bullet}$ is to determine the anisotropy of the *g*-matrix, which reflects the symmetry properties of the primary donor. Furthermore, these parameters play a crucial role in the interpretation and correct simulation of the spin-polarized EPR spectra of the light-induced radical pair $[P_{865}^{+\bullet}\, Q_A^{-\bullet}]$.[6,7] At X-Band, (9−10 GHz), the frequency at which most EPR measurements are performed, the spectrum is a featureless Gaussian envelope dominated by unresolved proton hyperfine splitting.[8] To resolve the *g*-matrix it is necessary to perform the EPR experiment under high magnetic field conditions provided that the *g*-strain (or *g*-anisotropy) is small enough to allow the full spectral resolution of the (generally) rhombic EPR powder spectrum. Here, "high field" means that

$$\frac{\Delta g}{g_{\mathrm{iso}}} \gg \frac{\Delta B_{1/2}^{\mathrm{hfi}}}{B_0} \qquad (1)$$

is fulfilled with Δg, the differences between the principal elements of the *g*-matrix that need to be resolved; g_{iso}, the isotropic *g*-factor: $\Delta B_{1/2}^{\mathrm{hfi}}$, the hyperfine-broadened EPR line width; and B_0, the externally applied magnetic field. One strategy for obtaining higher spectral resolution is therefore to work with fully deuterated samples. Due to their reduced hyperfine broadening "high-field" conditions can be achieved at lower fields than with protonated material. Here, we report on high-field studies where the fields have been increased sufficiently to afford the necessary resolution even for protonated samples.

2. Experimental Section

Rb. sphaeroides R26 was grown anaerobically under red light in 1 L bottles. Cells were kept at −20 °C after harvesting. RCs were isolated as before, using LDAO as the detergent.[9] They were concentrated by membrane filtration (Centricon 30 concentrator) in several rounds. Each time, the solution was concentrated about 10-fold and diluted with fresh buffer 1:2, until the final concentration of 0.75 mM was reached. In the case of other detergents (β-octylglucoside and sulfobetaine) the detergent was exchanged on a DEAE cellulose column. After loading, the samples were first washed with Tris buffer (10 mM, pH 7.5), then with Tris buffer containing the respective detergent, and finally eluted with detergent buffer containing 200 mM NaCl. Concentration was performed by membrane filtration described above but with LDAO replaced by the respective detergent. The primary donor absorption band at room temperature appeared at 864 nm. Chemical oxidation was performed with 50 mM potassium ferricyanide under nitrogen atmosphere. The samples were either mixed with 60% glycerol or did not contain any cryoprotectant, and were quickly frozen to liquid nitrogen temperature after the oxidation step. During transfer to the spectrometer the samples remained frozen. They were inserted cold into the EPR probe which was pre-cooled to 10 K.

The high field EPR spectrometer used for the EPR measurements at 12 T is very similar to the one described by Muller et al.[10] and operates in a frequency range of 30 GHz−3 THz using several millimeter- and sub-millimeter wave sources, at fields ranging from 0 to 17 T. In the series of experiments described in this communication, we used a Gunn oscillator at 110 ± 3 GHz (AB Millimetre, Paris), equipped with a set of Schottky diode harmonic generators and high pass filters (AB Millimetre), making it possible to work at higher harmonics. The fundamental frequency was measured using an EIP 578B counter. The magnet used for the 330 GHz experiments was an Oxford Instruments Teslatron consisting of a main set of superconducting coils which can be put in persistent mode in the vicinity of resonance and a smaller superconducting sweep coil operating in nonpersistent mode and allowing a field sweep of ±0.1 T with respect to the persistent field.

A 25 T resistive magnet (Keck magnet) with high homogeneity (10 ppm over a sphere of 1 cm without shimming, 1 ppm with shimming) suitable for magnetic resonance experiments has become available for use at the NHFML. The stability of the power supply that meets the magnet's requirements of up to 19.5 MW is extremely good (1 ppm RMS fluctuations) and allows the measurement of line widths of the order of 0.1−0.2 mT. The higher harmonics of the solid state sources needed to obtain the extremely high operating frequency at this magnetic field were too weak and could not be used. Instead we have used a CO_2-pumped far-IR laser with the laser gases methanol and methyl iodide as the excitation source, with lines available at 525 and 670 GHz, respectively. Using a bath cryostat, temperature control was possible between 4.2 and 100 K.

The spectrometer was operated in "single pass" mode with the sample placed within a Teflon cup (i.d. = 8 mm, height = 7 mm) inside an oversized stainless steel waveguide contained in an Oxford Instruments CF 1200 continuous flow cryostat. The temperature of the sample can be controlled from 4.2 to 300 K. A liquid helium-cooled hot-electron bolometer is used as a power detector to measure the absorption through the sample. The spectra are recorded in the first derivative mode, using magnetic field modulation at frequencies in the range of 1−10 kHz.

Field calibration and *g*-factor determination was performed as previously described using Mn^{2+} (0.05%) in MgO as a standard.[11] From sweeps taken over the entire Mn^{2+} spectral range (not shown), we can obtain a linearity of our field sweep (main coil in persistent mode) of better than 500 μT/50 mT, corresponding to an accuracy of approximately 0.05 mT within the sweep range of the primary donor radical cation spectrum. Previously, the accuracy of the calibration against the Mn^{2+} was limited by the Mn^{2+} line widths at low temperature.[11] With repeated heating/pumping cycles, however, it is possible to achieve line widths of ∼10.1 mT for the Mn-standard even at cryogenic temperatures, which increases the absolute accuracy of the calibration. The absolute error obtained using this calibration method is estimated as being of the order of $\delta g = \pm 5 \times 10^{-5}$. For the relative errors of the *g*-values (errors in the determination of Δg) we estimate a value of $\delta \Delta g = \pm 2 \times 10^{-5}$.

To obtain the anisotropic *g*-matrix the spectrum was simulated with a powder average, using (a) the SIMFONIA package supplied by Bruker Instruments Inc., and (b) a home-written simulation program.

3. Results and Discussion

Figure 1 shows the EPR spectra of chemically oxidized RCs from *Rb. sphaeroides* R26 at 11.9 T (330 GHz) and 23.9 T

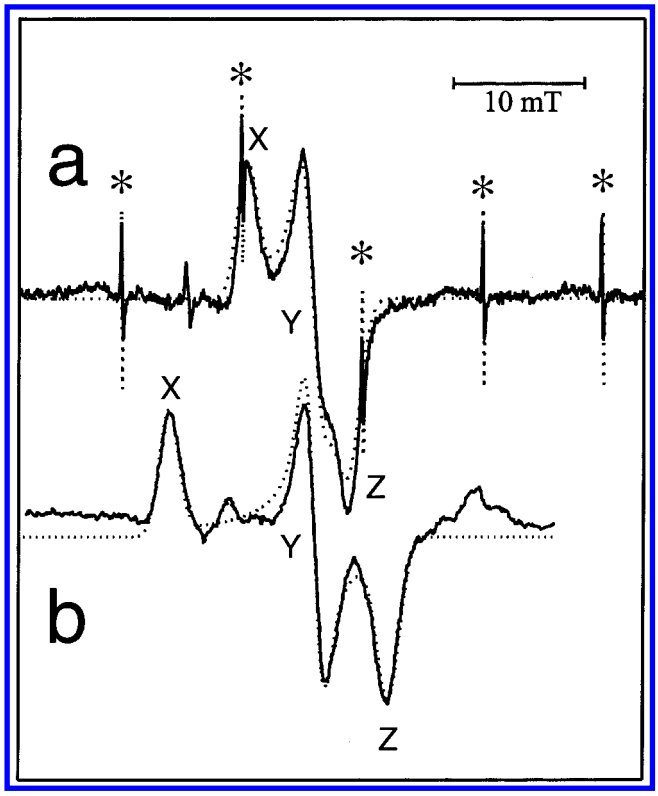

Figure 1. EPR spectra of the primary donor radical cation in *Rb. sphaeroides* R26 RCs at different magnetic field strengths at 10 K. The principal components of the *g*-matrix (g_{xx}, g_{yy}, and g_{zz}) are marked by X, Y, and Z for both spectra.(a) 327.690 GHz, solid line is the experimental spectrum, dashed line is the simulation. The sharp lines marked with asterisks arise from the MgO:Mn standard used for field calibration as described in the text. The center field is at 11.68015 T. Temperature was 10 K. Far-IR power was 3 mW, field modulation was 0.25 mT at 8 kHz. (b) 670.463 GHz, solid line is the experimental spectrum, dashed line is the simulation. The center field is at 23.92745 T. The simulation was carried out based on the same standard used as for (a). The spectrum does not show the lines of the Mn standard because it was added afterward and a separate spectrum taken. Temperature was 20 K. Far-IR power was 7 mW, field modulation was 0.25 mT at 8 kHz.

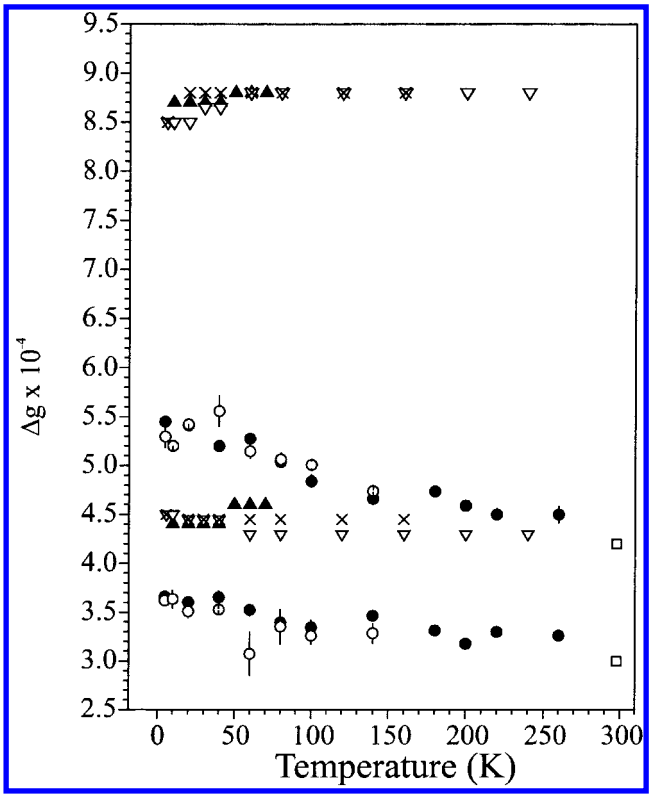

Figure 2. Temperature dependence of the $P_{865}^{+\bullet}$ Δg's as a function of temperature, compared with similar data from $P_{700}^{+\bullet}$.[11] For $P_{700}^{+\bullet}$ the filled circles (●) indicate that the measurements were made using Triton X-100 preparations of PS I RCs, and the open circles (○) indicate a digitonin preparation. The Δg-values obtained by Prisner et al.[32] on deuterated PS I are shown as open squares (□) for comparison at 296 K. The Δg-values obtained for $P_{865}^{+\bullet}$ in LDAO without glycerol are shown as open triangles pointing down (▽) for the data obtained at 330 GHz and as filled triangles pointing up (▲) for the data at 670 GHz. Data for the RCs in LDAO with glycerol at 330 GHz are presented with crosses (×). In all cases the lower of the two values (data points around $\Delta g \sim 4.5 \times 10^{-4}$ for the bacterial RCs and between 3.0 and 3.8×10^{-4} for PS I) correspond to $\Delta g_{yy-zz} = g_{yy} - g_{zz}$. The higher values (above 4.5×10^{-4}) correspond to $\Delta g_{xx-yy} = g_{xx} - g_{yy}$.

(670 GHz). The highest field was obtained with a custom-built Bitter magnet providing up to 25 T with high homogeneity. This spectrum (Figure 1 **b**) shows excellent resolution, where g_{yy} and g_{zz} are completely resolved unlike at lower frequencies (Figure 1 **a**). We also observed extraneous Mn^{2+}, easily identified by its sextet pattern in the spectrum (only partially shown in Figure 1 **b**), which had not been seen previously at 330 GHz (there are actually some very broad and weak features in the spectrum in Figure 1 **a** that could be due to Mn^{2+}). It has long been recognized by workers in the field that high-field EPR becomes extremely sensitive to Mn^{2+} with increasing fields which may be due to a field-dependent term in the fine structure-induced line width as demonstrated in a study on the aqueous manganous ion in frozen solutions.[12] It is well-known that the high-spin iron present in native RCs can easily be replaced by other divalent metal ions from the medium, such as Mn^{2+}.[13] Mn^{2+} from the growth medium may have been incorporated into the iron-binding site, and may be responsible for the extraneous signal that is visible due to the increased sensitivity at the higher frequency. Of course, Mn could also be bound in the Zn(II)-binding site, recently discovered by Utschig et al.[14]

The results of spectral simulations are shown in Figure 1, giving the following *g*-values: $g_{xx} = 2.00323$, $g_{yy} = 2.00241$, and $g_{zz} = 2.00197$ with an error interval of $\delta g = \pm 5 \times 10^{-5}$. Unlike the results obtained for $P_{700}^{+\bullet}$,[11] the *g*-values do not appear to be temperature dependent within our error margins, and spectra at higher temperatures could also be fitted using the same set of values (see Figure 2). A very small reduction in the *g*-anisotropy might be perceived as temperatures are lowered from 50 to 5 K, but the changes are just barely larger than the error margins ($\delta\Delta g = \pm 2 \times 10^{-5}$). This temperature insensitivity was observed irrespective of the presence or absence of glycerol as cryoprotectant, and was furthermore confirmed for RC preparations using the detergents β-octylglucoside and the zwitterionic N-(*n*-alkyl)-*N*,*N*-dimethyl-3-ammonio-1-propane sulfonate (sulfobetaine) SB12 (Sigma) instead of LDAO between 20 and 160 K (data not shown). Further tests on light-induced (instead of chemically oxidized) $P_{865}^{+\bullet}$ in the same preparations gave exactly the same results. The apparent insensitivity of the *g*-values to temperature in RCs of *Rb. sphaeroides* is surprising given that other spectroscopic parameters react quite strongly to temperature and have been interpreted as due to temperature-induced changes in geometric and electronic structure:

(i) The absorption band of the primary donor P_{865} shifts to the red (to approximately 890 nm) upon cooling.[15] This spectral shift has been interpreted in terms of structural changes in the dimer, i.e., an expansion of the special pair at higher temperatures[16] with a concomitant decrease of exciton coupling.[17]

(ii) Temperature-dependent changes also occur in the vibrational spectrum of P_{865}, in particular in the low-frequency region, where intra-dimer modes play a role and may be coupled to the primary charge separation.[18]

(iii) Magnetooptical difference spectroscopy (MODS) suggested the existence of two different conformations of the special pair with different absorption maxima, the temperature-dependent shift in the near-infrared absorption thus being due to the interconversion between them.[19]

(iv) The temperature dependence of the fine structure parameters of the primary donor triplet state is quite pronounced with $|D|$ becoming more monomeric at higher temperatures.[20,21] This was explained by a temperature-dependent admixture of a higher lying primary donor triplet state.

(v) The most detailed account of two distinct conformations of the primary donor radical cation was given by Lubitz et al. based on 2D ESEEM and ENDOR spectroscopy.[4,22] These two conformations may also be distinguished by the spectral position of the primary donor absorption band, and can be controlled by the polarity of the detergents used.[23,24] RCs prepared with the detergent LDAO show a temperature-dependent conversion between the two conformations between 160 K and room temperature[22] with the low temperature state characterized by a very asymmetric 5:1 spin density distribution over the dimer. Its formation can be affected by the addition of cryoprotectants such as glycerol.[22] It was expected that the *g*-anisotropy should reflect at least some of these changes in the dimer configuration. That is apparently not the case, as our data clearly show.

The simplest interpretation of this result is that the principal values of the *g*-matrixes of the bacterial primary donor radical cation remain the same as those of the monomeric $BChl^{+\bullet}$ radical cation within experimental error. This has been shown to be the case, albeit in an experiment with lower resolution.[25,26] However, the comparison between the homo-dimer mutant *Rb. sphaeroides* R26 and its hetero-dimer equivalent HL (M202), which features a monomeric radical cation in a comparable environment, demonstrated that the monomeric *g*-matrix is slightly more isotropic than the dimeric one.[25] The observed differences between the monomeric and dimeric case, especially for Δg_{yy-zz}, are large enough for us to be easily observable with the increased resolution at 670 GHz.

Another interpretation is that at cryogenic temperatures the main conformation of the primary donor radical cation in the various preparations used is the asymmetric dimer (5:1 spin density distribution) in accordance with the 2D ESEEM results by Käss et al.[4] We confirmed this independently by performing pulsed ENDOR experiments in X-band on the light-induced samples up to 100 K (data not shown). We are thus looking at a mostly monomeric radical cation (at least at temperatures below 100 K), located primarily on D_A (or P_L in the nomenclature of Müh et al.[22] This is consistent with the 1.14 mT line width we observed in X-band.[22] The radical should then be appropriately labeled $P_{850}^{+\bullet}$ according to the blue shift of the NIR absorption band that apparently accompanies this conformation,[23,24] although our starting material absorbed at 864 nm at room temperature. In this (monomeric) conformation, the *g*-matrix may not be as sensitive to structural changes as for a more delocalized wave function, e.g., PS I where the asymmetry of $P_{700}^{+\bullet}$ has been determined by ESEEM and ENDOR to approximately 3:1.[28] If this interpretation were correct we would expect to see a change in the principal values of the *g*-matrix at temperatures above 160 K where Müh et al. find a more dimeric spin distribution with ENDOR.[22] This is not the case and raises the question whether *g*-factor data alone are able to distinguish between different electronic structures on the special pair. There is of course also the possibility that competing trends may lead to the observed temperature-insensitivity of the *g*-matrix principal components, e.g., structural changes vs changes in spin distribution. Changes in the relative orientation of the *g*-matrix relative to the molecular frame may actually be more revealing but, of course, require the use of single crystals. High field EPR at the frequencies used in this study should actually be extremely useful for such work due to the increased spectral resolution which allows us to distinguish with much higher accuracy between the different sites in complex unit cells.

TABLE 1: *g*-factor Anisotropy of the Primary Donor Cation Radical in *Rb. Sphaeroides* R26, Its Hetero-Dimer Mutant HL (M202), and the Monomeric BChl $a^{+\bullet}$

	$(g_{xx}-2)\times 10^5$	$(g_{yy}-2)\times 10^5$	$(g_{zz}-2)\times 10^5$	$\Delta g_{xx-yy}\times 10^5$	$\Delta g_{xx-zz}\times 10^5$	ref
$P_{865}^{+\bullet}$	323(5)	241(5)	197(5)	82(2)	44(2)	this work
	329(3)	239(3)	203(3)	90(6)	36(6)	[26][a]
	329(3)	239(3)	208(3)	90(6)	31(6)	[26][a,b]
	333(2)	246(3)	204(3)	87(5)	42(6)	[27]
	330(10)	250(10)	210(10)	80(20)	40(20)	[25]
	334	246	221	88	25	[29]
	402	224	159	178	65	[30]
HL (M202)	319(2)	246(4)	215(4)	73(6)	31(8)	[27]
	325(5)	247(5)	219(5)	78(10)	28(10)	[27][a]
BChl $a^{+\bullet}$	330(10)	260(10)	220(10)	70(20)	40(20)	[25]

[a] Single-crystal work. [b] Fully deuterated RCs.

The primary donor cation of the RC from *Rb. sphaeroides* has been studied previously with high field EPR by several independent research groups using W and D band[26,27,29,30] (see Table 1). The values reported by Klette et al.[26] are in reasonable agreement with our data within the experimental error of $\delta g = \pm 5 \times 10^{-5}$. The g_{xx} and g_{zz} values reported by Wang et al.[29] are a little too high compared to our data which may be due to inadequate resolution at the magnetic fields used by these workers. It should be noted that the *g*-matrix values reported by Gulin et al.[30] differ significantly from those cited above. We consider these values with a total Δg_{xx-zz} of 0.00243 (three times the Δg_{xx-zz} reported here) unreliable because they are not consistent with other published data including previous Q-band spectra of deuterated RCs which, although still unresolved, show approximately only half this spectral width.[31]

One of the most striking findings of our experiments is that there is negligible *g*-strain in the primary donor radical cation. The line widths used for successful simulations of the high field spectra were between 1.1 and 1.4 mT (lines broadened at lower temperatures) and did not have to be increased for the simulations of the spectra taken at 670 GHz. This signals a remarkable homogeneity of the primary donor in our sample quite unlike the spectra of oxidized monomeric chlorophyll species in frozen organic solvents where *g*-strain dominates the line width above 300 GHz (data were obtained for Chl $a^{+\bullet}$ and will be published elsewhere). If the lack of *g*-strain is typical for other bio-organic radicals embedded in protein, high-field EPR up to and beyond the THz region may be possible and will prove to become extremely useful for the elucidation of the electronic structure, not only of photosynthetic RCs but also of other radical-generating enzymes as well. Preliminary results on the photosynthetic RC of *Heliobacterium chlorum* indicate that this is the case for the primary donor cation radical there as well, although 670 GHz does not give enough resolution for a full decomposition of the *g*-matrix of this more symmetric Chl dimer.

Another important aspect of this work is that it proves the

possibility for orientationally selective ENDOR at high magnetic fields which will allow the determination of anisotropic hyperfine coupling constants that otherwise can only be obtained by tedious single-crystal work. Such experiments are currently in progress in our laboratory.

Acknowledgment. This work was supported by the National High Magnetic Field Laboratory. The high-field Bitter magnet (up to 25 T with high homogeneity) was funded by the Keck foundation. L.C.B. acknowledges the support from the Human Frontiers in Science program (HFSPO Grant RGO349). The work in Gainesville was supported by NSF (Grant DMR-9601864). We thank Dr. Oleg Poluektov for the gift of the MgO:Mn standard.

Abbreviations

CW: Continuous Wave
ENDOR: Electron Nuclear DOuble Resonance
EPR: Electron Paramagnetic Resonance
ESEEM: Electron Spin−Echo Envelope Modulation
LDAO: lauryl-dimethyl-amine-*N*-oxide
P_{865}: Primary donor special pair
HFC: Hyperfine Coupling Constant
PS I: Photosystem I
Rb.: *Rhodobacter*
RC: Reaction Center
NHMFL: National High Magnetic Field Laboratory

References and Notes

(1) Deisenhofer, J.; Michel, H. *Annu. Rev. Cell Biol*. **1991**, *7*, 1−23.
(2) Yeates, T. O.; Komiya, H.; Chirino, A.; Rees, D. C.; Allen, J. P.; Feher, G. *Proc. Natl. Acad. Sci., U.S.A.* **1988**, *85*, 7993−7997.
(3) Feher, G. *J. Chem. Soc., Perkin Trans. 2* **1992**, 1861−1874.
(4) Käss, H.; Rautter, J.; Bönigk, B.; Höfer, P.; Lubitz, W. *J. Phys. Chem*. **1995**, *99*, 436−448.
(5) Hoff, A. J. In *The Photosynthetic Reaction Center*; Deisenhofer, J., Norris, J. R., Eds.; Academic Press: San Diego, 1993; Vol. 2, pp 331−386.
(6) van der Est, A.; Prisner, T.; Bittl, R.; Fromme, P.; Lubitz, W.; Möbius, K.; Stehlik, D. *J. Phys. Chem. B* **1997**, *101*, 1437−1443.
(7) Utschig, L. M.; Greenfield, S. R.; Tang, J.; Laible, P. D.; Thurnauer, M. C. *Biochemistry* **1997**, *36*, 8548−8558.
(8) Norris, J. R.; Uphaus, R. A.; Crespi, H. L.; Katz, J. J. *Proc. Natl. Acad. Sci. U.S.A.* **1971**, *68*, 625−628.
(9) Struck, A.; Cmiel, E.; Katheder, I.; Schäfer, W.; Scheer, H. *Biochim. Biophys. Acta* **1992**, *1101*, 321−328.
(10) Muller, F.; Hopkins, M. A.; Coron, N.; Grynberg, M.; Brunel, L.-C.; Martinez, G. *Rev. Sci. Instrum*. **1989**, *60*, 3681.
(11) Bratt, P. J.; Rohrer, M.; Krzystek, J.; Evans, M. C. W.; Brunel, L.-C.; Angerhofer, A. *J. Phys. Chem. B* **1997**, *101*, 9686−9689.
(12) Bellew, B. F.; Halkides, C. J.; Gerfen, G. J.; Griffin, R. G.; Singel, D. J. *Biochemistry* **1996**, *35*, 12186−12193.
(13) Debus, R. J.; Feher, G.; Okamura, M. Y. *Biochemistry* **1986**, *25*, 2276−2287.
(14) Utschig, L. M.; Ohigashi, Y.; Thurnauer, M. C.; Tiede, D. M. *Biochemistry* **1998**, *37*, 8278−8281.
(15) Kirmaier, C.; Holten, D. *Photosyn. Res*. **1987**, *13*, 225−260.
(16) Won, Y.; Friesner, R. A. *J. Phys. Chem*. **1988**, *92*, 2208−2214.
(17) Thompson, M. A.; Zerner, M. C.; Fajer, J. *J. Phys. Chem*. **1991**, *95*, 5693−5700.
(18) Cherepy, N. J.; Shreve, A. P.; Moore, L. J.; Boxer, S. G.; Mathies, R. A. *Biochemistry* **1997**, *36*, 8559−8566.
(19) Lous, E. J.; Hoff, A. J. *Photosyn. Res.* **1986**, *9*, 89−101.
(20) Hoff, A. J.; Proskuryakov, I. I. *Chem. Phys. Lett*. **1985**, *115*, 303−310.
(21) Aust, V.; Angerhofer, A.; Parot, P. H.; Violette, C. A.; Frank, H. A. *Chem. Phys. Lett.* **1990**, *173*, 439−442.
(22) Müh, F.; Rautter, J.; Lubitz, W. *Biochemistry* **1997**, *36*, 4155−4162.
(23) Wang, S.; Lin, S.; Lin, X.; Woodbury, N. W.; Allen, J. P. *Photosyn. Res*. **1994**, *42*, 203−215.
(24) Rautter, J.; Lendzian, F.; Lubitz, W.; Wang, S.; Allen, J. P. *Biochemistry* **1994**, *33*, 12077−12084.
(25) Burghaus, O.; Plato, M.; Rohrer, M.; Möbius, K.; MacMillan, F.; Lubitz, W. *J. Phys. Chem*. **1993**, *97*, 7639−7647.
(26) Klette, R.; Törring, J. T.; Plato, M.; Möbius, K.; Bönigk, B.; Lubitz, W. *J. Phys. Chem*. **1993**, *97*, 2015−2020.
(27) Huber, M.; Törring, J. T. *Chem. Phys*. **1995**, *194*, 379.
(28) Käss, H.; Bittersmann-Weidlich, E.; Andréasson, L.-E.; Bönigk, B.; Lubitz, W. *Chem. Phys*. **1995**, *194*, 419−432.
(29) Wang, W.; Belford, R. L.; Clarkson, R. B.; Davis, P. H.; Forrer, J.; Nilges, M. J.; Timken, M. D.; Walczak, T.; Thurnauer, M. C.; Norris, J. R.; Morris, A. L.; Zhang, Y. *Appl. Magn. Reson*. **1994**, *6*, 195−215.
(30) Gulin, V. I.; Dikanov, S. A.; Tsvetkov, Y. D.; Evelo, R. G.; Hoff, A. J. *Pure Appl. Chem*. **1992**, *64*, 903−906.
(31) Feezel, L. L.; Gast, P.; Smith, U. H.; Thurnauer, M. C. *Biochim. Biophys. Acta* **1989**, *974*, 149−155.
(32) Prisner, T. F.; McDermott, A. E.; Un, S.; Norris, J. R.; Thurnauer, M. C.; Griffin, R. G. *Proc. Natl. Acad. Sci. U.S.A.* **1993**, *90*, 9485−9488.